Electronic Supplementary Information for

Solvent-responsive cavitand lanthanum complex

Francesca Guagnini,[a] Alessandro Pedrini,[a] Timothy M. Swager,[b] Chiara Massera,[a] Enrico Dalcanale[a]**

[a] Dipartimento di Scienze Chimiche, della Vita e della Sostenibilità Ambientale and INSTM UdR Parma, Università di Parma, Parco Area delle Scienze 17/A, 43123 Parma (PR), Italy

[b] Department of Chemistry and Institute for Soldier Nanotechnologies, Massachusetts Institute of Technology, 77 Massachusetts Avenue, Cambridge, Massachusetts 02139, United States

Table of contents

1. NMR spectra

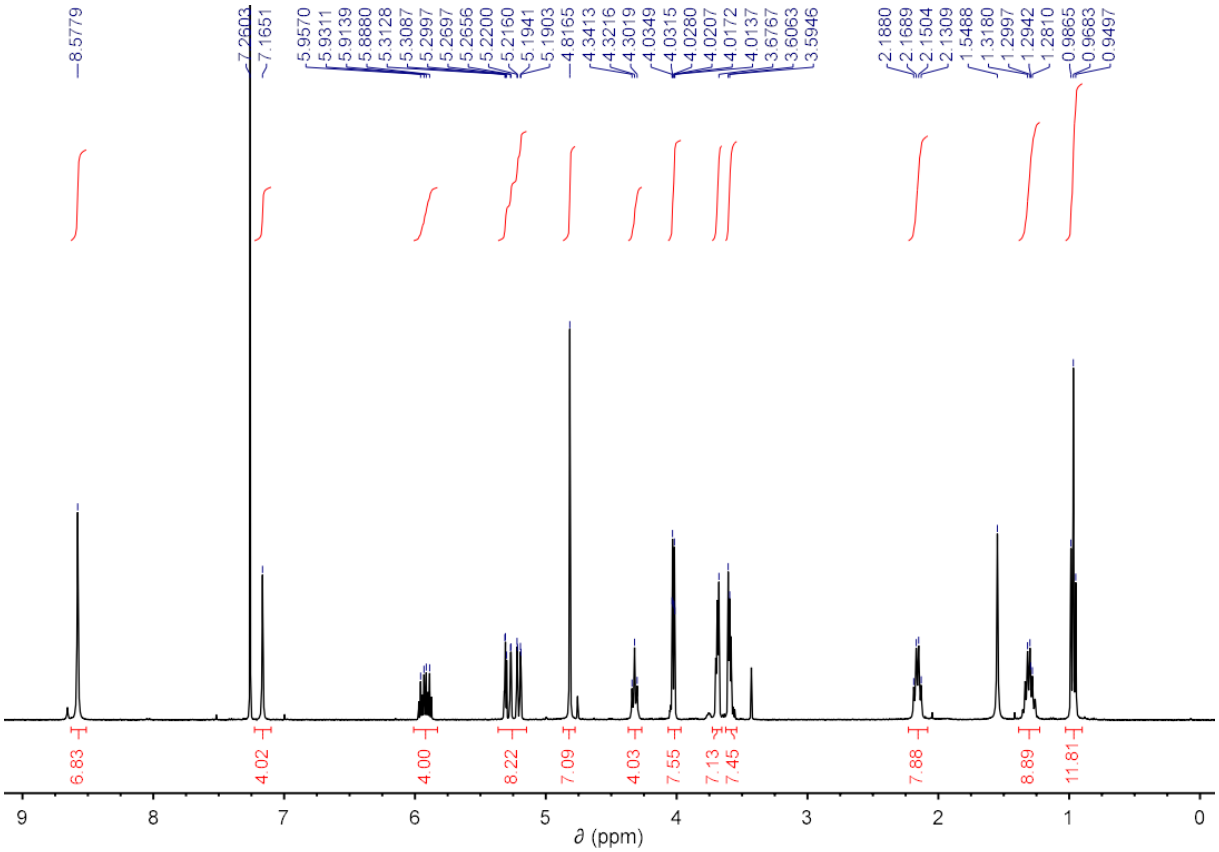

Figure S1. ^{1}H NMR ($CDCl_3$, 400 MHz, 298 K) of resorcinarene **II**.

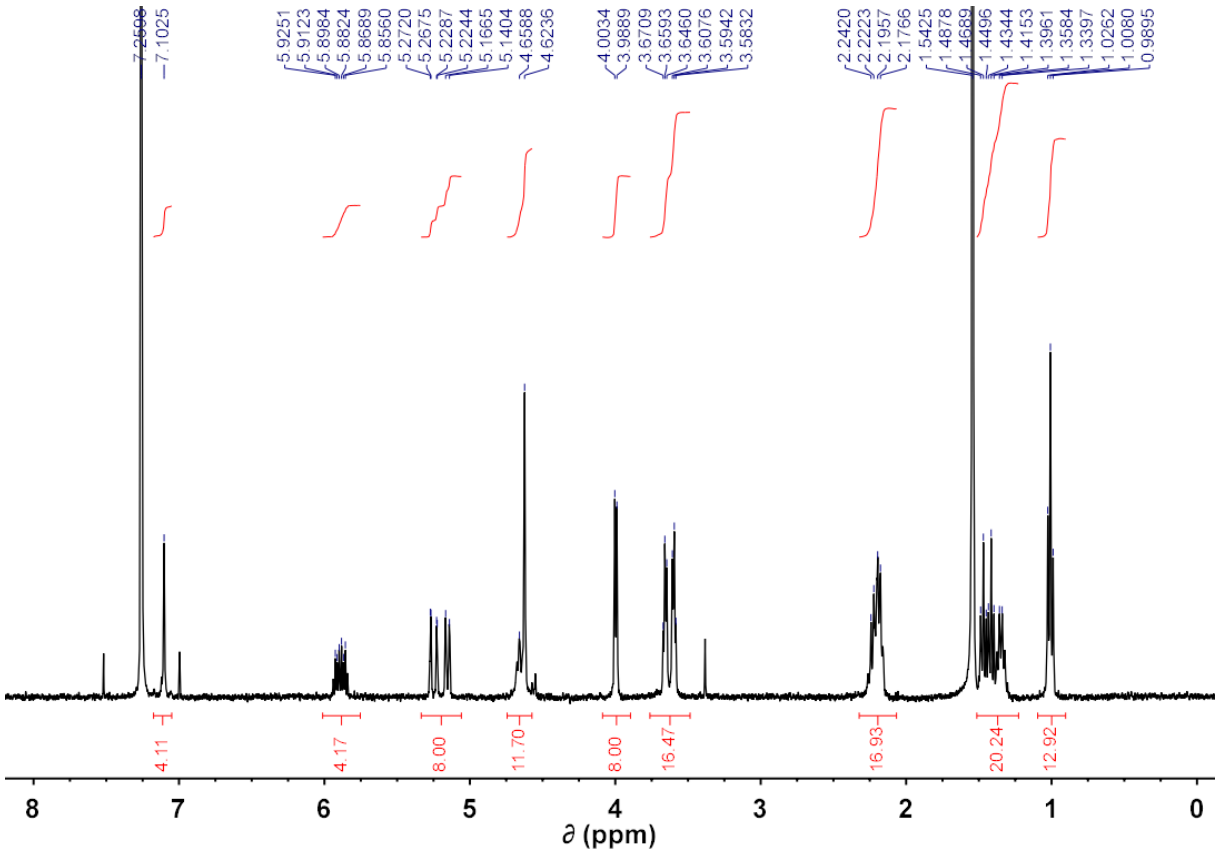

Figure S2. ^{1}H NMR ($CDCl_3$, 400 MHz, 298 K) of tetraphosphonate cavitand **III**.

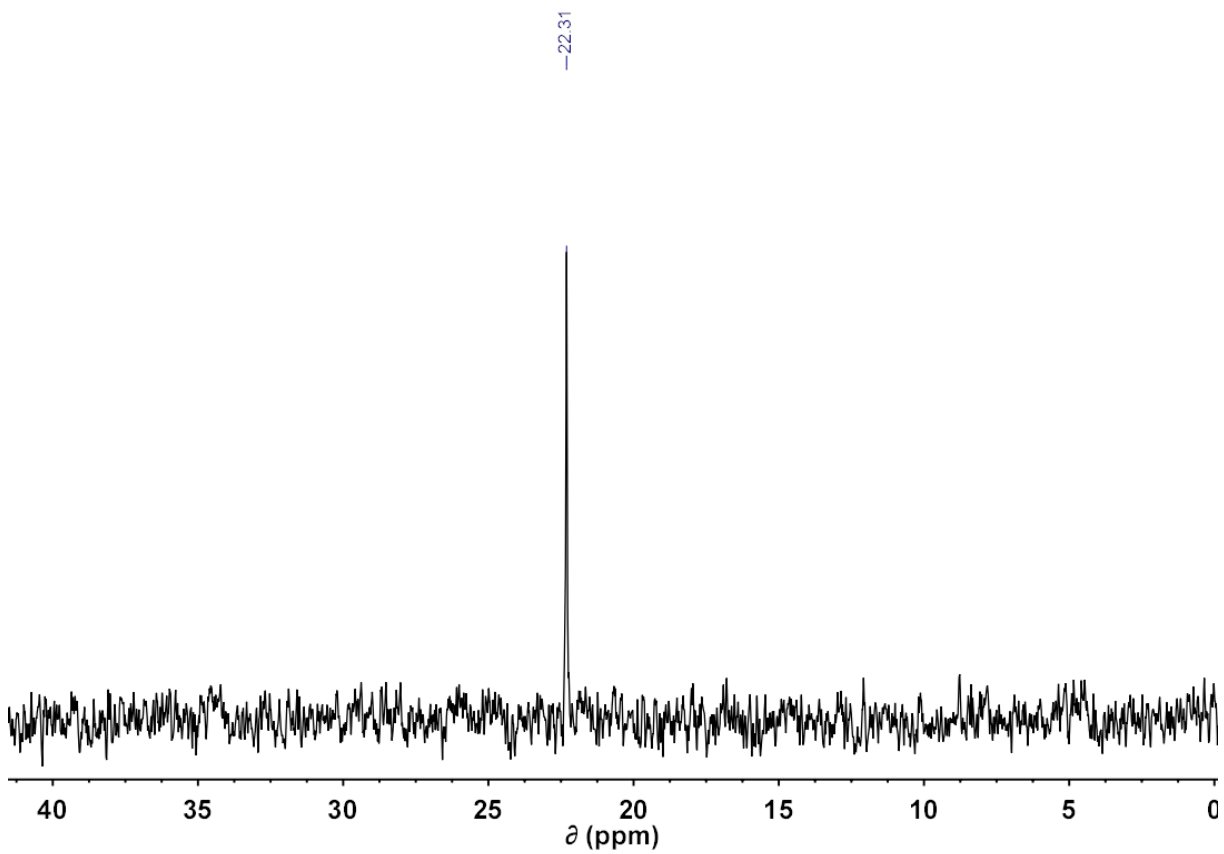

Figure S3. ^{31}P NMR ($CDCl_3$, 162 MHz, 298 K) of tetraphosphonate cavitand **III**.

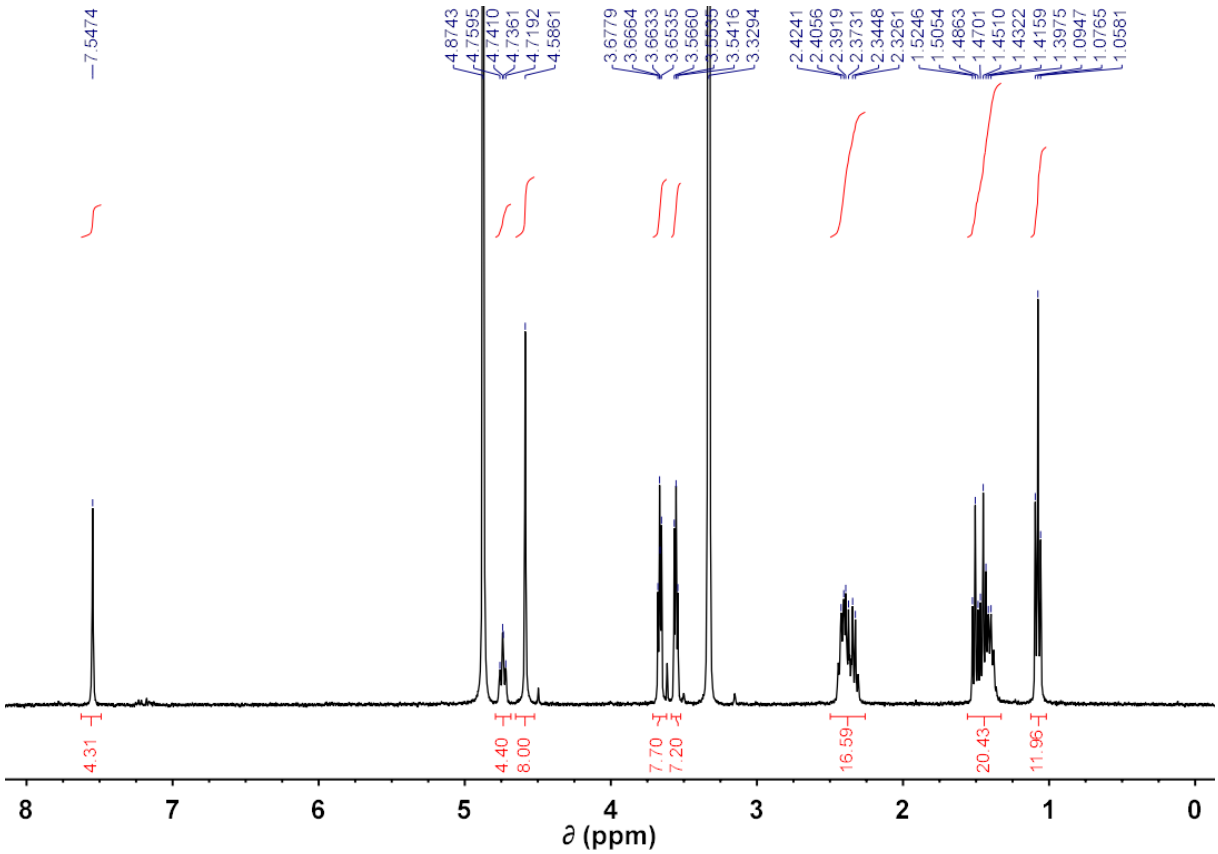

Figure S4. ^{1}H NMR (CD_3OD, 400 MHz, 298 K) of tetraphosphonate cavitand **1**.

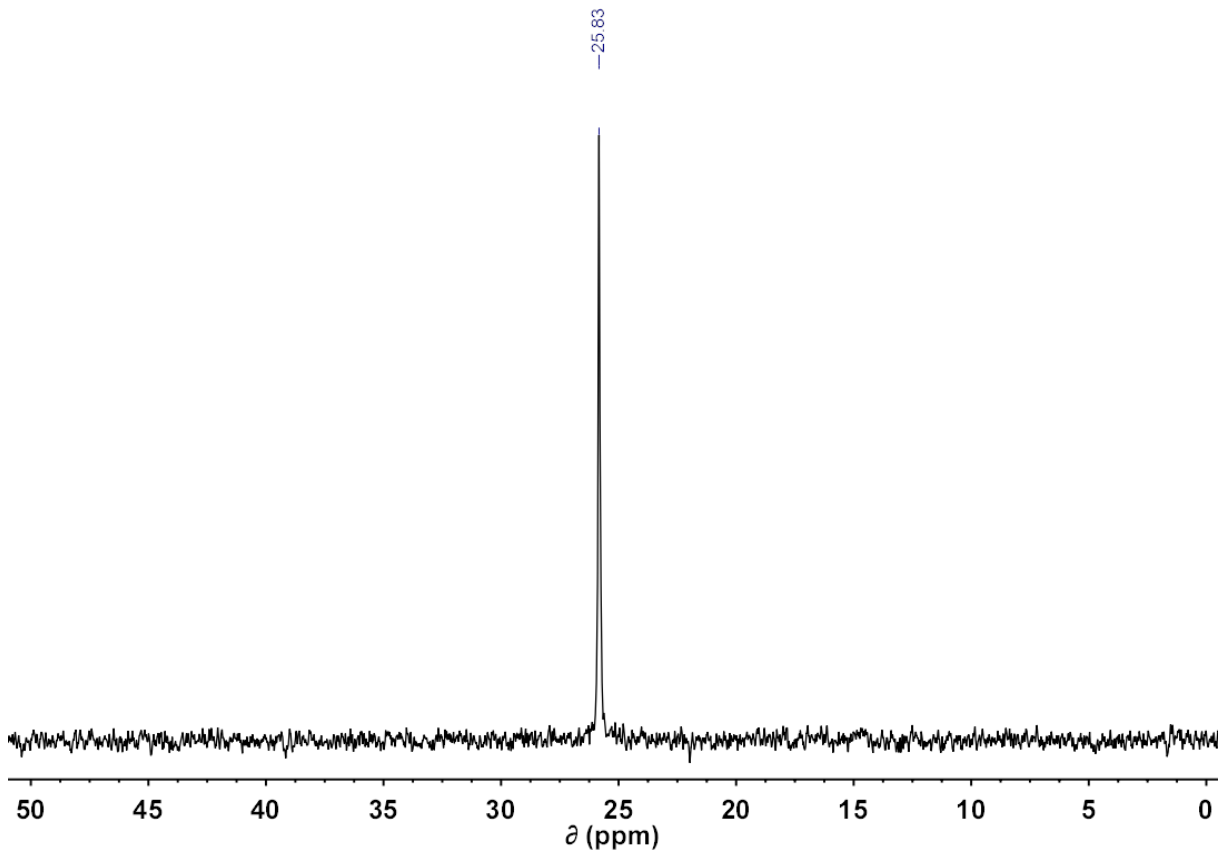

Figure S5. ^{31}P NMR (CD_3OD, 162 MHz, 298 K) of tetraphosphonate cavitand **1**.

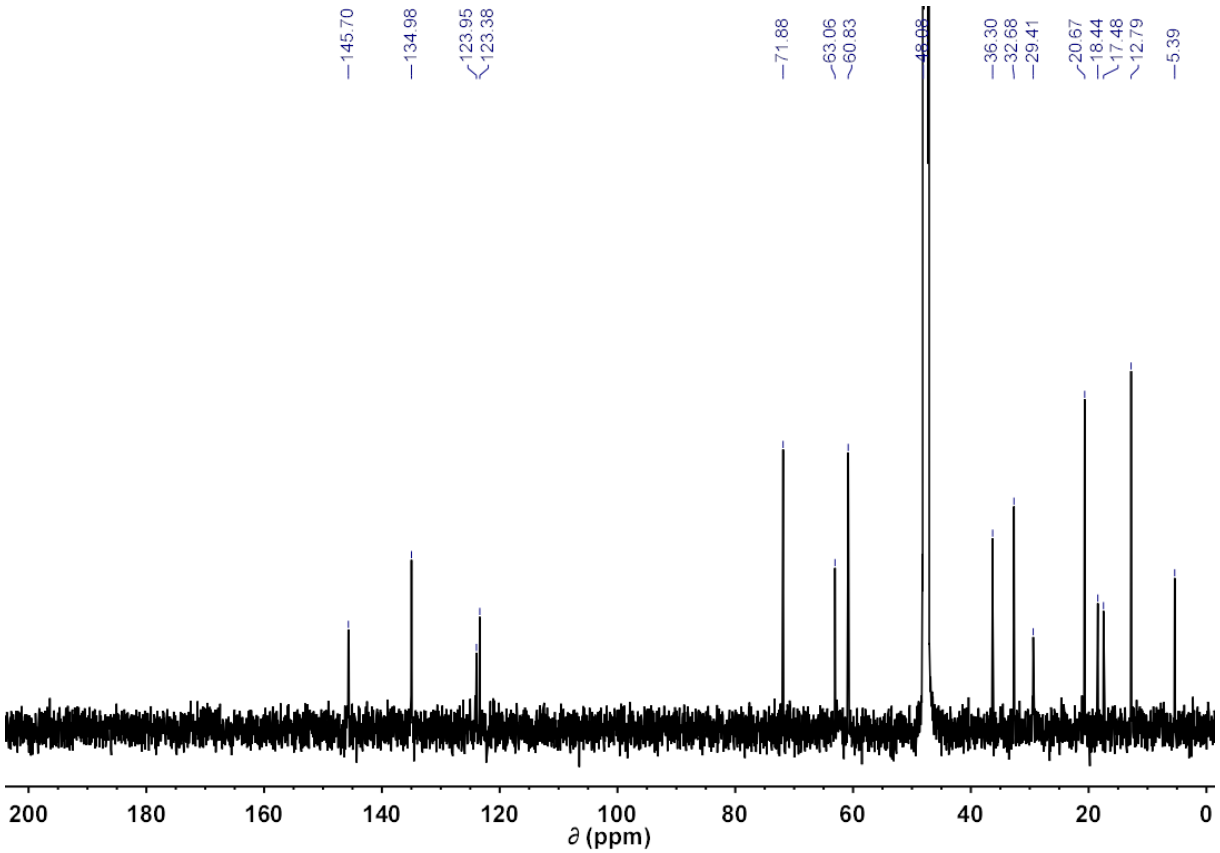

Figure S6. ^{13}C NMR (CD_3OD, 100 MHz, 298 K) of tetraphosphonate cavitand **1**.

2. ITC experiments

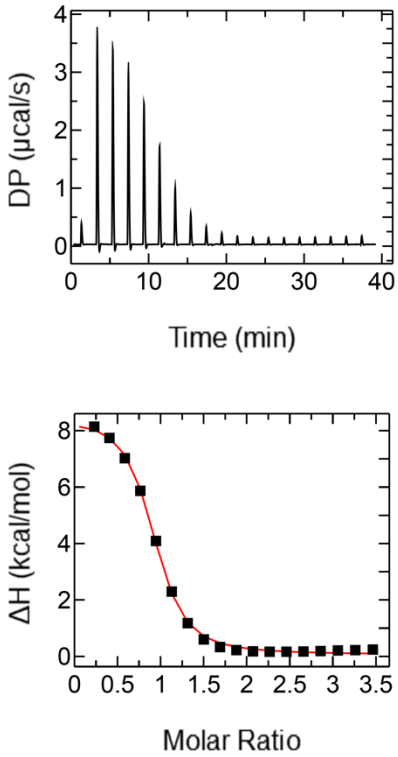

Figure S7. ITC titration of 1 and $LaCl_3$ in acetonitrile; [cavitand] = 2.07 mM; [$LaCl_3$] = 0.12 mM.

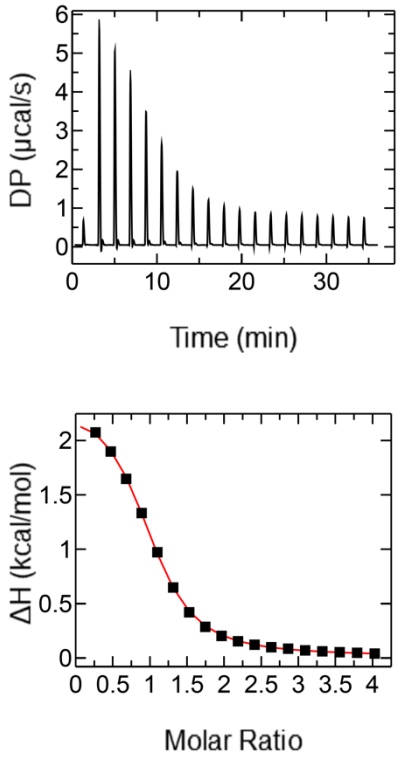

Figure S8. ITC titration of 1 and $LaCl_3$ in acetone; [cavitand] = 11.1 mM; [$LaCl_3$] = 0.54 mM.

3. X-Ray Crystallography

Table S1. Crystallographic data for La-**1**

Formula	$C_{68}H_{116}Cl_3LaN_4O_{30}P_4$
Formula weight	1838.78
Crystal system	Triclinic
Space group	*P*-1
a/Å	14.6516(2)
b/Å	15.3311(3)
c/Å	20.0375(5)
α/°	92.916(1)
β/°	95.482(1)
γ/°	92.327(1)
V/Å^3	4469.9(2)
Z	2
D_c/g cm^{-3}	1.366
F(000)	1920
μ/mm^{-1}	0.715
$\theta_{min,max}$/°	2.501-28.285
Reflections collected	59535
Independent reflections	20927 [R(int) = 0.0519]
Observed reflections	16270
Data/restr./param.	20927 / 6 / 1073
S^a	1.015
R[$Fo>4\sigma(Fo)$]^b	0.0498
wR_2^b	0.1248
$\Delta\rho_{min,max}$/e Å^{-3}	2.064, -1.479

[a]Goodness-of-fit $S = [\Sigma w(F_o^2-F_c^2)^2/(n-p)]1/2$, where n is the number of reflections and p the number of parameters. [b]$R_1 = \Sigma \| F_o | - | F_c \| / \Sigma | F_o |$, $wR_2 = [\Sigma[w(F_o^2 F_c^2)^2]/\Sigma[w(F_o^2)^2]]^{1/2}$.

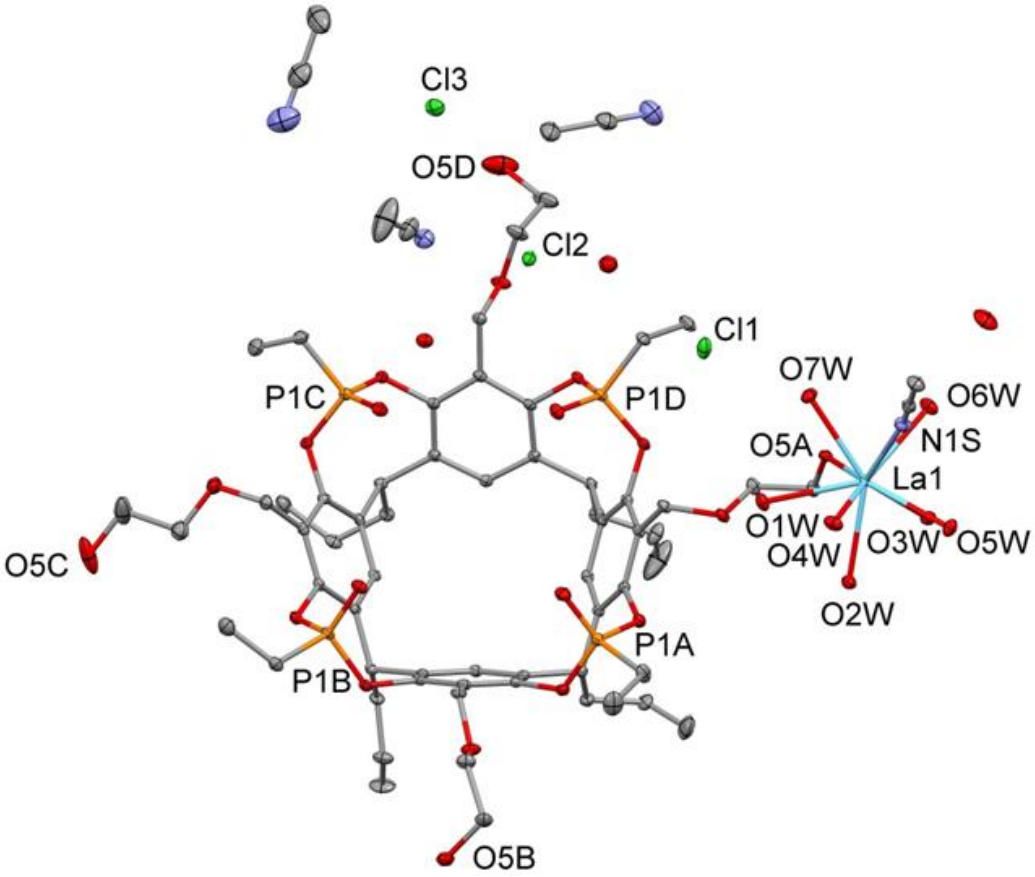

Figure S9. Ortep view of La-**1** with partial atom labelling scheme and displacement ellipsoids drawn at the 20% probability level. H atoms have been omitted for clarity.

Table S2. Selected bond lengths (Å) in La-**1**.

La1-N1S	2.732(4)	La1-O4W	2.529(3)
La1-O5A	2.537(2)	La1-O5W	2.523(3)
La1-O1W	2.542(3)	La1-O6W	2.511(3)
La1-O2W	2.529(4)	La1-O7W	2.513(3)
La1-O3W	2.632(3)		

Table S3. H bonding parameters (Å, °) in La-**1**.

Donor-H	**Donor···Acceptor**	**H···Acceptor**	**Donor-H···Acceptor**
O1W-H2W 0.854(3)	O1W···O4A 2.814(4)	H2W···O4A 1.97(3)	O1W-H2W···O4A 170.2(2)
O7W-H14W 0.807(9)	O7W···Cl1 3.162(3)	H14W···Cl1 2.37(8)	O7W-H14W···Cl1 165.9(9)
O8W-H15W 0.800	O8W···Cl2 3.216(3)	H15W···Cl2 2.47	O8W-H15W···Cl2 157
O8W-H16W 0.800	O8W···O3C 2.700(4)	H16W···O3C 1.92	O8W-H16W···O3C 163
O10W-H19W 0.800	O10W···Cl1 3.179(4)	H19W···Cl1 2.39	O10W-H19W···Cl1 168
O10W-H20W 0.800	O20W···Cl2 3.200(3)	H20W···Cl2 2.44	O10W-H20W···Cl2 168
O9W-H17W 0.800	O9W···O3B^{i} 2.841(4)	H17W···O3B^{i} 2.06	O9W-H17W···O3B^{i} 167
O2W-H4W 0.76(5)	O2W···O10W^{i} 2.762(5)	H4W···O10W^{i} 2.00(9)	O2W-H4W···O10W^{i} 178(5)
O4W-H7W 0.98(6)	O4W···O3D^{i} 2.713(4)	H7W···O3D^{i} 1.74(6)	O4W-H7W···O3D^{i} 171(2)
O7W-H13W 0.66(6)	O7W···O3A^{i} 2.729(5)	H13W···O3A^{i} 2.09(7)	O7W-H13W···O3A^{i} 165(4)
O1W-H1W 0.849(3)	O1W···Cl1^{i} 3.117(3)	H1W···Cl1^{i} 2.272(1)	O1W-H1W···Cl1^{i} 173.2(2)

O5W-H10W 0.872(3)	O5W···O8W^{i} 2.707(4)	H10W···O8W^{i} 1.931(3)	O5W-H10W···O8W^{i} 147.5(2)
O4W-H8W 0.77(7)	O4W···O10W^{i} 3.378(5)	H8W···O10W^{i} 2.78(7)	O4W-H8W···O10W^{i} 134(7)
O4W-H8W 0.77(7)	O4W···Cl2^{i} 3.330(3)	H8W···Cl2^{i} 2.64(7)	O4W-H8W···Cl2^{i} 151(6)
O5W-H9W 0.872(3)	O5W···Cl2^{ii} 3.101(3)	H9W···Cl2^{ii} 2.352(1)	O5W-H9W···Cl2^{ii} 144.1(2)
O2W-H3W 0.98(6)	O2W···O8W^{ii} 2.776(4)	H9W··· O8W^{ii} 1.78(6)	O2W-H3W···O8W^{ii} 174(5)
O3W-H6W 0.883(3)	O3W··· Cl3^{ii} 3.091(3)	H6W··· Cl3^{ii} 2.220(1)	O3W-H6W···Cl3^{ii} 168.5(2)
O6W-H11W 0.871(3)	O6W··· Cl3^{ii} 3.124(3)	H11W··· Cl3^{ii} 2.310(1)	O6W-H11W···Cl3^{ii} 155.7(2)
O5C-H5C 0.840(7)	O5C··· Cl3^{iii} 3.068(7)	H5C··· Cl3^{iii} 2.251(1)	O5C-H5C···Cl3^{iii} 164.6(5)
O5B-H5OB 0.840(3)	O5B··· Cl1^{iii} 3.083(3)	H5OB··· Cl1^{iii} 2.287(1)	O5B-H5OB···Cl1^{iii} 158.2(2)
O9W-H18W 0.800	O9W··· N2Si^{v} 2.980(7)	H18W··· N2Si^{v} 2.23	O9W-H18W···N2Si^{v} 155

i = -x+1,-y,-z+1; ii = x-1,+y,+z; iii = x,+y-1,+z; iv = -x+1,-y+1,-z+1

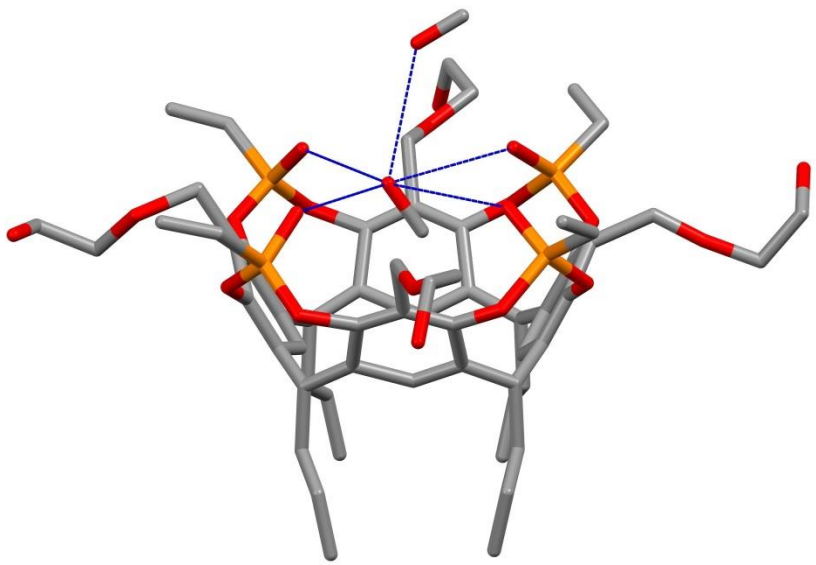

Figure S10. Molecular structure of cavitand **1** crystallized by slow evaporation of a solution of La-**1** in methanol. The H-bond pattern is shown as blue dashed lines.

Main crystallography data for cavitand 1 ($C_{60}H_{84}P_4O_{20}\cdot 2CH_3OH$): Monoclinic, C2/m, a = 14.068(1) Å, b = 23.176(2) Å, c = 24.274(2) Å, β = 93.678(3)°, V = 7898.1(11) $Å^3$, Z = 8. Theta range for data collection: 2.322 to 17.284°. Reflections collected / unique: 32510 / 2496 [R(int) = 0.1176].

4. Radius Models

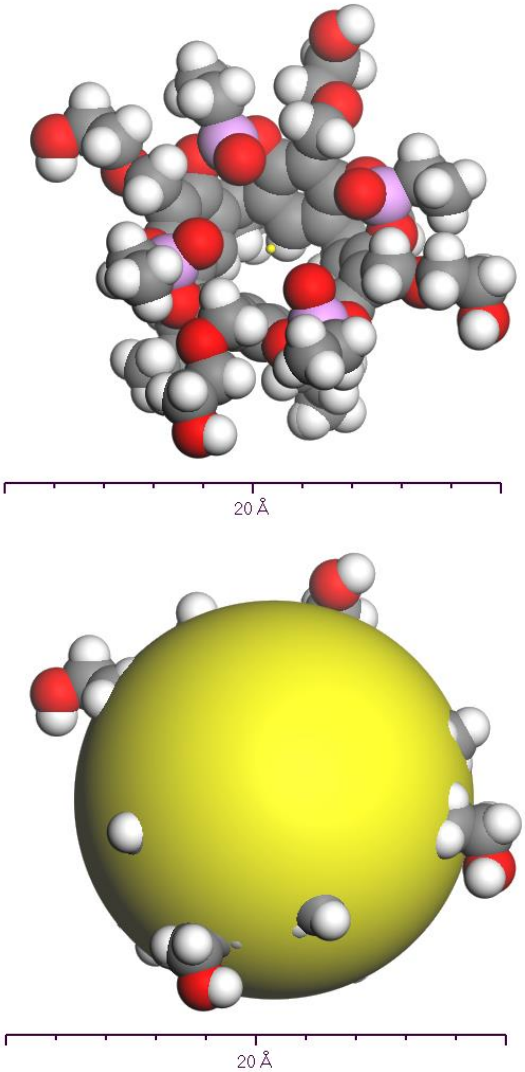

Figure S11. (top) Space-filling model for cavitand **1** showing calculated centroid (yellow dot); (bottom) sphere grown from the centroid with a radius of 8 Å.

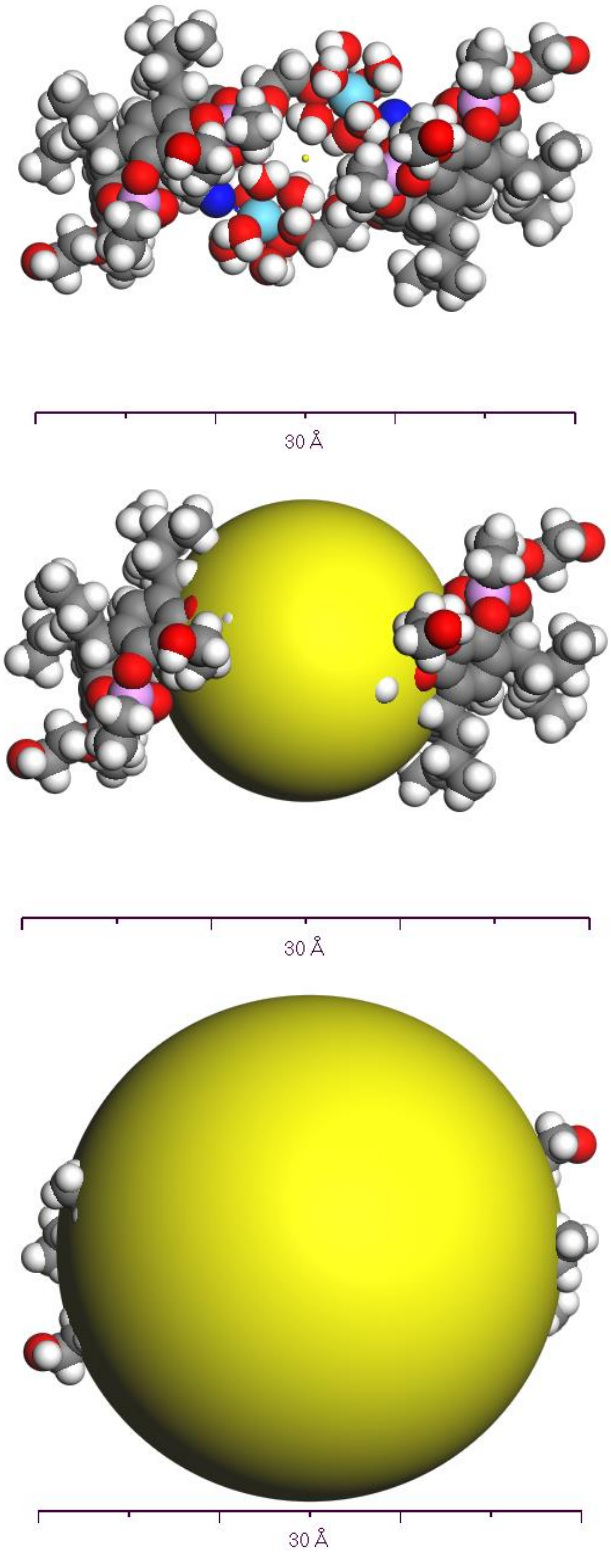

Figure S12. (top) Space-filling model for La-**1** dimer showing calculated centroid (yellow dot); (middle) sphere grown from the centroid with a radius of 8 Å; (bottom) sphere grown from the centroid with a radius of 14 Å.

5. 1D NMR study of solvent responsiveness

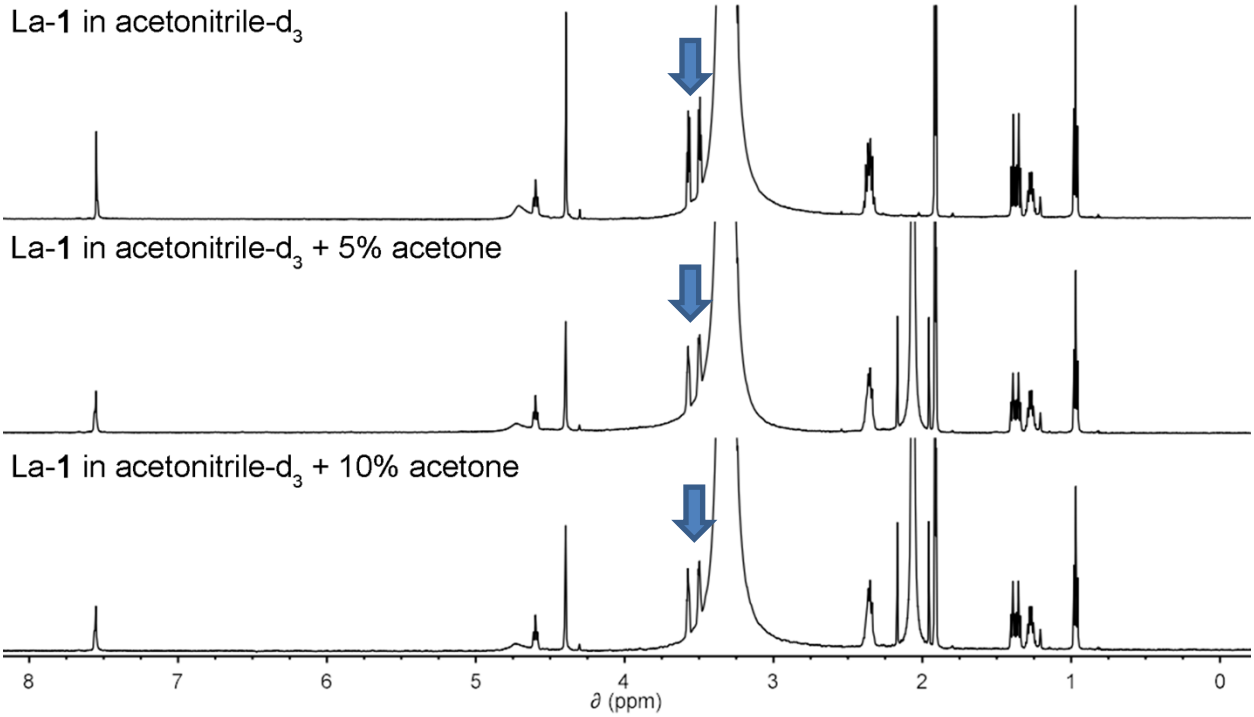

Figure S13. ^{1}H NMR spectra of La-**1** complex in acetonitrile-d_3 before (top) and after the addition of 5% (middle) and 10% (bottom) of acetone. The broadening of the signals related to the coordinating glycol units are evidenced by the arrows.